

## Electrochemistry

International Edition: DOI: 10.1002/anie.201601615  
German Edition: DOI: 10.1002/ange.201601615

## Solvent-Mediated Control of the Electrochemical Discharge Products of Non-Aqueous Sodium–Oxygen Electrochemistry

Iain M. Aldous and Laurence J. Hardwick\*

**Abstract:** The reduction of dioxygen in the presence of sodium cations can be tuned to give either sodium superoxide or sodium peroxide discharge products at the electrode surface. Control of the mechanistic direction of these processes may enhance the ability to tailor the energy density of sodium–oxygen batteries ( $\text{NaO}_2$ :  $1071 \text{ Wh kg}^{-1}$  and  $\text{Na}_2\text{O}_2$ :  $1505 \text{ Wh kg}^{-1}$ ). Through spectroelectrochemical analysis of a range of non-aqueous solvents, we describe the dependence of these processes on the electrolyte solvent and subsequent interactions formed between  $\text{Na}^+$  and  $\text{O}_2^-$ . The solvents ability to form and remove  $[\text{Na}^+\text{-O}_2^-]_{\text{ads}}$  based on Gutmann donor number influences the final discharge product and mechanism of the cell. Utilizing surface-enhanced Raman spectroscopy and electrochemical techniques, we demonstrate an analysis of the response of  $\text{Na-O}_2$  cell chemistry with sulfoxide, amide, ether, and nitrile electrolyte solvents.

Intensive research into lithium–oxygen ( $\text{Li-O}_2$ ) batteries in recent years has led to the study of alternative alkali-metal–oxygen cell chemistries.<sup>[1]</sup> The inclusion of other alkali metals in the research of energy storage devices beyond lithium ion batteries is merited by enhancing sustainability, yet still providing striking theoretical values for specific energy ( $\text{Na-O}_2$   $1505 \text{ Wh kg}^{-1}$   $\text{K-O}_2$   $1100 \text{ Wh kg}^{-1}$ ). The possible reduced oxygen discharge products for  $\text{M-O}_2$  electrochemistry include superoxide ( $\text{MO}_2^-$ ), peroxide ( $\text{M}_2\text{O}_2$ ), and oxide ( $\text{M}_2\text{O}$ ;  $\text{M}$  = alkali metal) species.<sup>[2]</sup> With the exception of one recent study detecting  $\text{LiO}_2$ ,<sup>[3]</sup> the main discharge product of  $\text{Li-O}_2$  is  $\text{Li}_2\text{O}_2$ .<sup>[4]</sup> However for  $\text{Na-O}_2$  batteries, both  $\text{Na}_2\text{O}_2 \cdot 2\text{H}_2\text{O}$ <sup>[5]</sup> and  $\text{NaO}_2$ <sup>[1b,6]</sup> have been reported, along with  $\text{KO}_2$ <sup>[1a]</sup> for  $\text{K-O}_2$  batteries.

Although well documented for  $\text{Li-O}_2$ ,<sup>[7]</sup>  $\text{Na-O}_2$  electrolytes have thus far been limited to carbonate, ether, and the ionic liquid (IL) *N*-methyl-*N*-propylpiperidinium bis(trifluoromethylsulfonate) imide ( $\text{PP}_{13}\text{TFSI}$ )-based electrolytes.<sup>[6a,d]</sup> Carbonate and the IL have been shown to be unstable electrolytes for  $\text{NaO}_2$ .<sup>[8]</sup> Carbonate-based electrolytes were initially shown to

give  $\text{Na}_2\text{O}_2$  as the discharge product, however sodium carbonate and carboxylates have now been detected more recently, and thought to be the major discharge product.<sup>[8]</sup> These observations match the behavior observed in  $\text{Li-O}_2$  cells cycled in organic carbonates as the main solvent.<sup>[6d]</sup> Glyme-based electrolytes; including tetraethylene glycol dimethyl ether (TEGDME) and diethylene glycol dimethyl ether (DEGDME) have shown evidence of  $\text{NaO}_2$ ,  $\text{Na}_2\text{O}_2$ , and  $\text{Na}_2\text{O}_2 \cdot \text{H}_2\text{O}$  products.<sup>[6a,8]</sup> One major aspect of metal– $\text{O}_2$  battery enquiries is the inducement of a solution-based mechanism to enhance discharge capacity.<sup>[6a,9]</sup> This is achieved through the solvation of superoxide or control of the Lewis acidity of the alkali metal cation, and thus the strength of alkali-metal–superoxide interactions.<sup>[9b,10]</sup>

Solvation of superoxide through controlled water content increases discharge product size, including toroidal  $\text{Li}_2\text{O}_2$ <sup>[9a]</sup> and cubic  $\text{NaO}_2$ .<sup>[6a,11]</sup> Further understanding of this process in  $\text{Na-O}_2$  has established that the electrolyte acidic proton content promotes the formation of  $\text{HO}_2$  radicals as a phase transfer catalyst.<sup>[6a,12]</sup> According to Xia et al.,<sup>[6a]</sup>  $\text{HO}_2$  enables the removal of superoxide from the surface above 5 ppm  $\text{H}_2\text{O}/\text{H}^+$  content and a subsequent solution metathesis reaction with  $\text{Na}^+$  creates  $\text{NaO}_2$  nuclei that precipitate on the electrode surface. Similarly, a recent study by Jirkovsky et al.<sup>[13]</sup> stated that even small amounts of water (10–16 ppm) enhances the oxygen reduction reaction (ORR) kinetics. The suggested mechanism defined the role of water as an active part of surface intermediates, through hydrogen bonding to  $\text{LiO}_2$ , which promotes the formation of  $\text{Li}_2\text{O}_2$  and the resulting partial dissociation of  $\text{H}_2\text{O}$  to  $\text{HO}_2$  and  $\text{OH}^-$ .<sup>[13]</sup> Superior discharge capacity has been demonstrated with benzoic and acetic acid in  $\text{Na-O}_2$ , along with phenol and ethanol in  $\text{Li-O}_2$ , providing additional evidence for this phenomenon.<sup>[6a,b]</sup>

In very dry electrolytes ( $\leq 10$  ppm), control of the Lewis acidity of the alkali metal cation through electrolyte solvation allows alkali-metal–superoxide ion pairs to form and react within the double layer to enhance discharge capacity.<sup>[9b]</sup> Once in solution,  $\text{LiO}_2$  may undergo a second electron addition or a chemical disproportionation reaction to form  $\text{Li}_2\text{O}_2$ . These observations were qualitatively compared to Gutmann donor number, whereby high donor number solvents, including dimethylsulfoxide (DMSO), are able to better support a solution-based mechanism enhancing battery capacity.<sup>[9b]</sup> Mid- and low-ranged donor number solvents lack the solvation power to support a solution-based mechanism.<sup>[9b]</sup> By utilizing in situ surface-enhanced Raman spectroscopy (SERS) as an interfacial probe, we investigated the effect of solvent donor number upon the oxygen reduction reaction (ORR) in the presence of sodium cations.

[\*] I. M. Aldous, Dr. L. J. Hardwick  
Department of Chemistry  
Stephenson Institute for Renewable Energy  
University of Liverpool  
Liverpool, L69 7ZF (UK)  
E-mail: hardwick@liverpool.ac.uk

Supporting information for this article can be found under:  
<http://dx.doi.org/10.1002/anie.201601615>.

© 2016 The Authors. Published by Wiley-VCH Verlag GmbH & Co. KGaA. This is an open access article under the terms of the Creative Commons Attribution License, which permits use, distribution and reproduction in any medium, provided the original work is properly cited.

A detailed electrochemical study is presented within the Supporting Information (Figures S1 and S2, Tables S1–S4). Variations in the CV response were observed that were dependent both on the electrode substrate and the solvent; however, limited mechanistic insights could be directly acquired. SERS data provides insight into surface species and intermediates. By applying this technique to each electrolyte system, it is apparent that solvent choice can strongly affect the identity of  $\text{Na}_x\text{O}_y$  species on planar roughened Au electrodes. Upon discharge, the high donor number solvents, DMSO and DMA, produced signals in the region for  $\text{O}_2^-$  and  $\text{NaO}_2$  (Figure 1 a,b and Table 1). This agrees with the electrochemical analysis for DMSO, in which only a small variation in the CV response is noted for the exchange of  $\text{TEA}^+$  with  $\text{Na}^+$ . The corresponding Raman spectra for systems in the absence of alkali metal cations only displayed a signal at  $1110\text{ cm}^{-1}$  for the O–O stretch of  $\text{O}_2^-$  adsorbed on the surface.<sup>[9b]</sup> There was little change in the spectra upon discharge after moving to DMA. The same formation of  $\text{O}_2^-$  and subsequent  $\text{NaO}_2$  formation was observed. A blue shift of approximately  $5\text{--}10\text{ cm}^{-1}$  was identified from the expected values of  $1110\text{ cm}^{-1}$  ( $\nu_{\text{O-O}}$ ,  $\text{O}_2^-$ ) and  $1156\text{ cm}^{-1}$  ( $\nu_{\text{O-O}}$ ,  $\text{NaO}_2$ ), denoting varying interactions of  $\text{O}_2^-$  and cation between different solvents.<sup>[9b,14]</sup>

**Table 1:** Raman bands for ORR discharge products/ $\text{cm}^{-1}$ .

	$\text{O}_2^-$ (Au- $\text{O}_2^-$ )	$\text{Na}_2\text{O}_2$ ( $736\text{ cm}^{-1}$ )	$\text{Na}_2\text{O}_2$ ( $792\text{ cm}^{-1}$ )	$\text{O}_2^-$ ( $\text{O}_2^-$ )	$\text{NaO}_2$ ( $1156\text{ cm}^{-1}$ )
DMSO	488	–	–	1107	1156
DMA	–	–	–	1119	1161
DEGDME	–	710	760	1109	–
MeCN	–	706	764	1108	–

Within these systems, superoxide initially forms in the presence of  $\text{Na}^+$ , as shown in Equations (1) and (2).



The addition of an electron to the surface-adsorbed  $\text{O}_2$  leads to the formation of superoxide that subsequently interacts with  $\text{Na}^+$  at the interface. This interaction is heavily dependent on the solvation of both  $\text{O}_2^-$  at the surface and the solvation of  $\text{Na}^+$ . These interactions control the acidity and basicity of the  $\text{Na}^+$  and  $\text{O}_2^-$ . The solvation shell in these cases will consist of anions ( $\text{O}_2^-$  and  $\text{OTf}^-$ ), cation ( $\text{Na}^+$ ), and

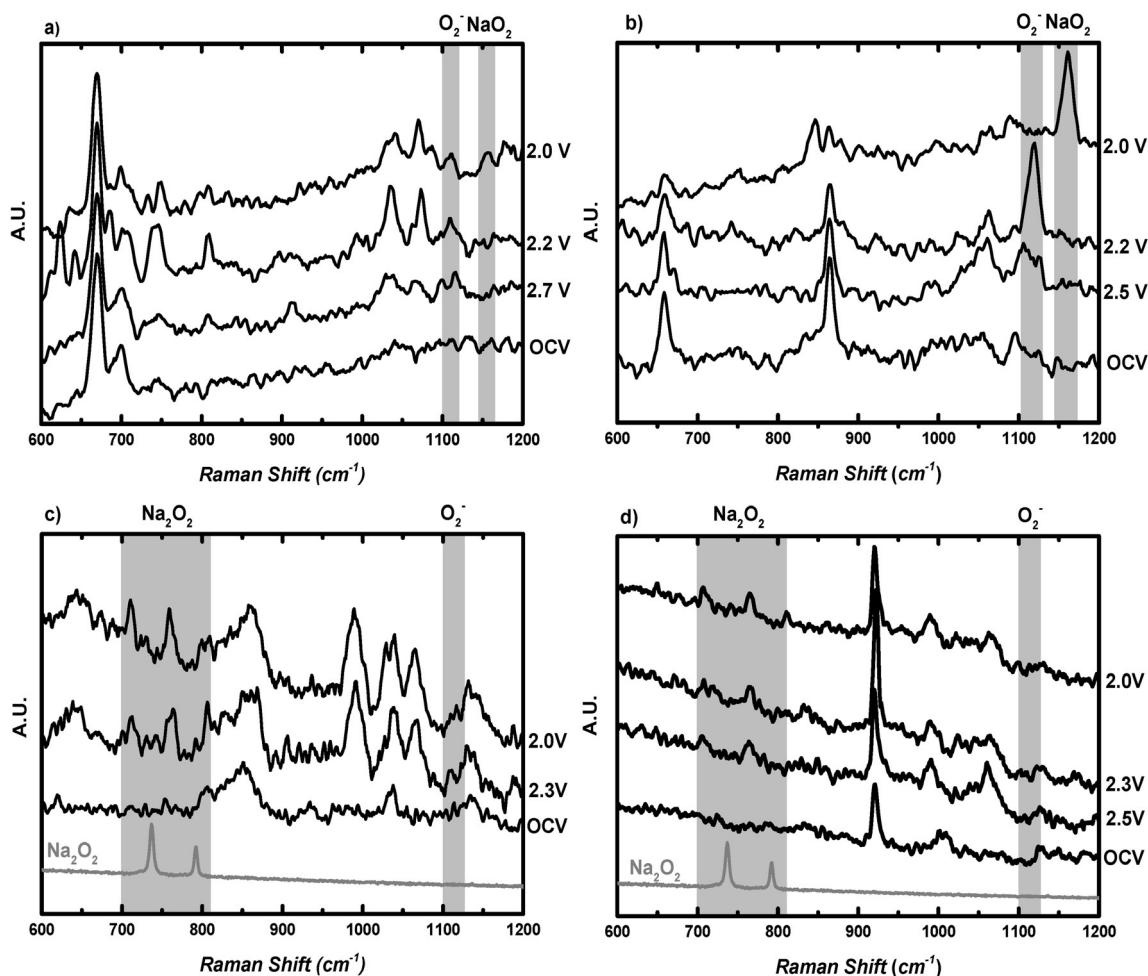


**Figure 1.** In situ SERS of oxygen-saturated 0.1 M NaOTf in a) DMSO, b) DMA, c) 1 M NaOTf in DEGDME, and d) 0.1 M NaOTf in MeCN and roughened Au working disc electrodes at  $23^\circ\text{C}$ ,  $0.1\text{ V s}^{-1}$  at varying potentials vs.  $\text{Na}^+/\text{Na}$ .

solvent molecules.<sup>[15]</sup> The OTf<sup>-</sup> presence is based on the solubility of the salt within each solvent, which induces the formation of contact, solvent-separated, and free ion pairs in solution.<sup>[16]</sup> In DMSO, the peak at 1032 cm<sup>-1</sup> (Table S5) splits at a potential of 2.0 V versus Na<sup>+</sup>/Na denoting ion pair formation, but does not observably affect the Na<sub>x</sub>O<sub>y</sub> peaks within the spectra.

The interaction between DMSO-solvated [Na<sup>+</sup>-O<sub>2</sub><sup>-</sup>] is highly favorable, allowing the interaction to be ascribed to an ion pair, which corresponds to the detection of the band at 1107 cm<sup>-1</sup>. This soluble species is easily removed from the surface, which explains the quasi-reversible nature of O<sub>2</sub> and Na<sup>+</sup> electrochemistry in DMSO. Furthermore, the detection of the signal for NaO<sub>2</sub> at 1156 cm<sup>-1</sup> is likely due to the aggregation and precipitation of NaO<sub>2</sub> on the surface as the reductive potential increases to 2.0 V versus Na<sup>+</sup>/Na. Multiple CV scans within 0.1 M NaOTf showed that the quasi-reversible process breaks down, and revealed the formation of two oxidation peaks within the initial cyclovoltammetric peak (Figure S3). This corroborated the initial ion pair formation, and the subsequent aggregation and precipitation of NaO<sub>2</sub> on the surface. As the number of CV sweeps increases, more time has been allowed for NaO<sub>2</sub> to precipitate, which leads to the growth of the second oxidation peak at 2.75 V versus Na<sup>+</sup>/Na.

A similar situation is induced by DMA-solvated NaOTf, but the change in donation from solvent to cation the Lewis acidity of sodium that may explain the distinct shift from [Na<sup>+</sup>-O<sub>2</sub><sup>-</sup>] to NaO<sub>2</sub> (1119 cm<sup>-1</sup> to 1161 cm<sup>-1</sup>) within the spectra. The mechanism here is considered to be as stated in Equations (1) and (2). This follows the removal of NaO<sub>2</sub> from the surface, subsequent electrolytic saturation within the double layer, and aggregation and precipitation of NaO<sub>2</sub> (Scheme 1). However, considering the water content of these systems (<20 ppm) and recent data by Xia et al.,<sup>[6a]</sup> the proposed inducement of this reaction through HO<sub>2</sub> formation should enhance the formation of cuboid NaO<sub>2</sub>. Therefore, solvents can induce the removal of Na<sub>x</sub>O<sub>y</sub> from the surface in a similar manner to how water can solvate and remove O<sub>2</sub><sup>-</sup> from the surface, as suggested by Xia et al.<sup>[6a]</sup> However, we have found no spectroscopic evidence, either indirect or directly, of the presence of H<sub>2</sub>O or HO<sub>2</sub>, as discussed in detail by both Xia et al.<sup>[6a]</sup> and Jirkovsky et al.<sup>[13]</sup>

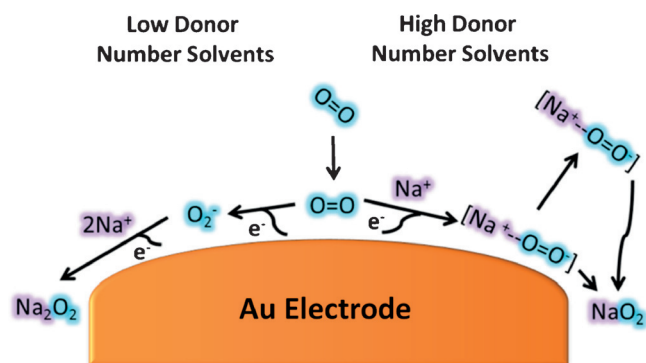
The poor conductivity of low concentration salt (0.1 M), DEGDMC-based electrolyte required that the Raman anal-

ysis be carried out at 1 M NaOTf in order to reduce significant overpotentials (Figure 1c). The SERS data showed that the main discharge product was Na<sub>2</sub>O<sub>2</sub>, based on the observation of a shifted doublet peak at 710 and 760 cm<sup>-1</sup>. This is in contrast to the majority of Na-O<sub>2</sub> cell observations on a number of bulk carbon electrodes in which NaO<sub>2</sub> is the major product identified.<sup>[6c,11,14,17]</sup> The detection of Na<sub>2</sub>O<sub>2</sub> rather than NaO<sub>2</sub> on a planar roughened gold electrode may be due to surface morphology as the current role of the surface is unclear in directing preferential formation of NaO<sub>2</sub> or Na<sub>2</sub>O<sub>2</sub>.<sup>[17a]</sup> DEGDMC is a medium donor number solvent that in Li-O<sub>2</sub> chemistry has been shown to support a solution-based mechanism and surface mechanism by increasing the longevity of LiO<sub>2</sub>. Here, it is believed that a different process is occurring. In this case, the lifetime and energetics of the ion pair of [Na<sup>+</sup>-O<sub>2</sub><sup>-</sup>] may increase the amount of Na<sub>2</sub>O<sub>2</sub> formed owing to the transfer of a second electron, but also owing to the kinetic and thermodynamic stability of the products.<sup>[17a]</sup> Na<sub>2</sub>O<sub>2</sub> has been shown to be the thermodynamically favorable product over NaO<sub>2</sub> above 10 μm.<sup>[17a]</sup>

MeCN-based electrolyte SERS data also displayed a doublet band at 714 and 767 cm<sup>-1</sup> that was assigned as Na<sub>2</sub>O<sub>2</sub> (Figure 1d). The absence of a NaO<sub>2</sub> signal indicated preferential Na<sub>2</sub>O<sub>2</sub> formation, suggesting that any initially formed NaO<sub>2</sub> is short-lived or that superoxide is solely present before a second electron transfer. Therefore, if a surface-bound NaO<sub>2</sub> film is present, then it rapidly grows beyond kinetic stability, allowing for a second electron reduction and a subsequent Na<sub>2</sub>O<sub>2</sub> discharge product.<sup>[17a]</sup> The increased Lewis acidity of Na<sup>+</sup> in MeCN causes the formation of a dense passivation film of Na<sub>2</sub>O<sub>2</sub>, which is comparable to the behavior observed in Li<sup>+</sup> in the same solvent (Figure S4). The assigned Na<sub>2</sub>O<sub>2</sub> signals here were shifted from our Raman standard. This is a similar case for DEGDMC (Figure 1c), which we will explain further below.

To confirm that the shifted bands assigned as Na<sub>2</sub>O<sub>2</sub> were due to reduced oxygen species, careful control SERS experiments were carried out. Electrolytes purged under Ar did not show any signals assigned to reduced O<sub>2</sub><sup>-</sup> species as above (Figure S5–S8). In the same spectral region as the higher Na<sub>2</sub>O<sub>2</sub> peak in the SERS data, there was a corresponding OTf<sup>-</sup> anion peak at 760 cm<sup>-1</sup> at OCV, however there are no peaks that appear around 710 cm<sup>-1</sup>. The OTf<sup>-</sup> band does not change in intensity under potential control, and so therefore this feature arises from Na<sub>2</sub>O<sub>2</sub> due to O<sub>2</sub> species. The presence of interfacial OTf<sup>-</sup> can be explained by the formation of ion pairs or aggregation of ion pairs at the interface. The doublet feature assigned to Na<sub>2</sub>O<sub>2</sub> is shifted to a lower wavenumber than expected. If this shift is due to H<sub>2</sub>O, then it would be expected to increase the signal to a higher wavenumber.<sup>[18]</sup> The strong presence of ion-pairs within the double layer may enhance the interaction of surface Na<sub>2</sub>O<sub>2</sub> and the OTf<sup>-</sup> anion, which could explain the observation of the red-shifted bands (by ca. 30 cm<sup>-1</sup>) of Na<sub>2</sub>O<sub>2</sub>.

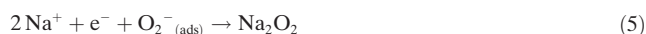
The formation of ion pairs was revealed by the appearance of a peak at 1040 cm<sup>-1</sup>. This region denotes the ν<sub>as</sub> SO<sub>3</sub>, which is considered the group within the anion that interacts with alkali metal cations.<sup>[16,19]</sup> The formation of ion-pairs interacting with Na<sup>+</sup> within Na<sub>2</sub>O<sub>2</sub> at the surface may cause



**Scheme 1.** Mechanism of oxygen reduction in non-aqueous solvents in the presence of Na<sup>+</sup> cations (with H<sub>2</sub>O ≤ 20 ppm).

this observed shift. These bands relating to ion-pair formation are detected in DMSO and DEGDME, suggesting that ion solvation may influence the discharge product.

Therefore, the SERS data provides spectroscopic evidence that the lack of solvation of  $O_2^-$  in low donor number solvents increases the proximity of  $O_2^-$ , allowing for a second electron reduction to form a thin passivating film of  $Na_2O_2$  [Eq. (4), (5)] (Scheme 1). This mechanism follows:



In conclusion, in situ SERS investigations have shown that solvent choice can influence the overall surface discharge product of Na- $O_2$  cell chemistry. Observable, yet shifted, SERS signals for  $Na_2O_2$  in low donor number solvents suggest that solvation of initially formed  $O_2^-$  is important in the control of this mechanism on Au electrodes. Higher solvation leads to the absence of  $Na_2O_2$  owing to initial formation of an ion pair between  $Na^+$  and  $O_{2(ads)}^-$ , which is removed from the surface and then aggregates and precipitates out later as  $NaO_2$  in the discharge process. Solvents with a lower ability to control the Lewis acidity of  $Na^+$  do not form an ion pair interaction with  $O_2^-$  and proceeds through a surface mechanism where, upon further oxygen reduction,  $Na_2O_2$  is preferentially formed at the interface.

## Acknowledgements

The authors would like to gratefully acknowledge the financial support from the Engineering and Physical Sciences Research Council (EPSRC), U.K., under grant number EP/J020265/1.

**Keywords:** oxygen reduction reaction · peroxides · sodium-oxygen batteries · superoxides · surface-enhanced Raman spectroscopy

**How to cite:** *Angew. Chem. Int. Ed.* **2016**, *55*, 8254–8257  
*Angew. Chem.* **2016**, *128*, 8394–8397

- [1] a) X. Ren, Y. Wu, *J. Am. Chem. Soc.* **2013**, *135*, 2923–2926; b) P. Hartmann, C. L. Bender, M. Vračar, A. K. Dürr, A. Garsuch, J. Janek, P. Adelhelm, *Nat. Mater.* **2013**, *12*, 228–232; c) K. M. Abraham, Z. Jiang, *J. Electrochem. Soc.* **1996**, *143*, 1–5.
- [2] K. M. Abraham, *J. Electrochem. Soc.* **2015**, *162*, A3021–A3031.
- [3] J. Lu, Y. Jung Lee, X. Luo, K. Chun Lau, M. Asadi, H.-H. Wang, S. Brombosz, J. Wen, D. Zhai, Z. Chen, D. J. Miller, Y. Sub Jeong, J.-B. Park, Z. Zak Fang, B. Kumar, A. Salehi-Khojin, Y.-K. Sun, L. A. Curtiss, K. Amine, *Nature* **2016**, 529, 377–382.
- [4] Z. Peng, S. A. Freunberger, L. J. Hardwick, Y. Chen, V. Giordani, F. Bardé, P. Novák, D. Graham, J.-M. Tarascon, P. G. Bruce, *Angew. Chem. Int. Ed.* **2011**, *50*, 6351–6355; *Angew. Chem.* **2011**, *123*, 6475–6479.
- [5] a) Y. Li, H. Yadegari, X. Li, M. N. Banis, R. Li, X. Sun, *Chem. Commun.* **2013**, 49, 11731–11733; b) Q. Sun, Y. Yang, Z.-W. Fu, *Electrochem. Commun.* **2012**, *16*, 22–25; c) H. Yadegari, Y. Li, M. N. Banis, X. Li, B. Wang, Q. Sun, R. Li, T.-K. Sham, X. Cui, X. Sun, *Energy Environ. Sci.* **2014**, *7*, 3747–3757; d) Y. C. Z. Jian, F. Li, T. Zhang, C. Liu, H. Zhou, *J. Power Sources* **2014**, *251*, 466–469.
- [6] a) C. Xia, R. Black, R. Fernandes, B. Adams, L. F. Nazar, *Nat. Chem.* **2015**, *7*, 496–501; b) B. D. McCloskey, J. M. Garcia, A. C. Luntz, *J. Phys. Chem. Lett.* **2014**, *5*, 1230–1235; c) P. Hartmann, C. L. Bender, J. Sann, A. K. Dürr, M. Jansen, J. Janek, P. Adelhelm, *J. Phys. Chem. Lett.* **2013**, *15*, 11661–11672; d) J. Kim, H.-D. Lim, H. Gwon, K. Kang, *Phys. Chem. Chem. Phys.* **2013**, *15*, 3623–3629.
- [7] a) D. Sharon, D. Hirsberg, M. Afri, A. Garsuch, A. A. Frimer, D. Aurbach, *J. Phys. Chem. C* **2014**, *118*, 15207–15213; b) Q. Yu, S. Ye, *J. Phys. Chem. C* **2015**, *119*, 12236–12250; c) S. A. Freunberger, Y. Chen, Z. Peng, J. M. Griffin, L. J. Hardwick, F. Bardé, P. Novák, P. G. Bruce, *J. Am. Chem. Soc.* **2011**, *133*, 8040–8047; d) S. A. Freunberger, Y. Chen, N. E. Drewett, L. J. Hardwick, F. Bardé, P. G. Bruce, *Angew. Chem. Int. Ed.* **2011**, *50*, 8609–8613; *Angew. Chem.* **2011**, *123*, 8768–8772; e) F. Bardé, Y. Chen, L. Johnson, S. Schaltin, J. Franssaer, P. G. Bruce, *J. Phys. Chem. C* **2014**, *118*, 18892–18898.
- [8] N. Zhao, X. Guo, *J. Phys. Chem. C* **2015**, *119*, 25319–25326.
- [9] a) N. B. Aetukuri, B. D. McCloskey, J. M. Garcia, L. E. Krupp, V. Viswanathan, A. C. Luntz, *Nat. Chem.* **2015**, *7*, 50–56; b) L. Johnson, C. Li, Z. Liu, Y. Chen, S. A. Freunberger, P. C. Ashok, B. B. Praveen, K. Dholakia, J.-M. Tarascon, P. G. Bruce, *Nat. Chem.* **2014**, *6*, 1091–1099.
- [10] C. O. Laoire, S. Mukerjee, K. M. Abraham, E. J. Plichta, M. A. Hendrickson, *J. Phys. Chem. C* **2009**, *113*, 20127–20134.
- [11] N. Ortiz-Vitoriano, T. P. Batcho, D. G. Kwabi, B. Han, N. Pour, K. P. C. Yao, C. V. Thompson, Y. Shao-Horn, *J. Phys. Chem. Lett.* **2015**, *6*, 2636–2643.
- [12] Z. Peng, Y. Chen, P. G. Bruce, Y. Xu, *Angew. Chem. Int. Ed.* **2015**, *54*, 8165–8168; *Angew. Chem.* **2015**, *127*, 8283–8286.
- [13] J. Staszak-Jirkovský, R. Subbaraman, D. Strmcnik, K. L. Harrison, C. E. Diesendruck, R. Assary, O. Frank, L. Kobr, G. K. H. Wiberg, B. Genorio, J. G. Connell, P. P. Lopes, V. R. Stamenkovic, L. Curtiss, J. S. Moore, K. R. Zavadil, N. M. Markovic, *ACS Catal.* **2015**, *5*, 6600–6607.
- [14] P. Hartmann, C. L. Bender, M. Vračar, A. K. Dürr, A. Garsuch, J. Janek, P. Adelhelm, *Nat. Mater.* **2013**, *12*, 228–232.
- [15] W. Huang, R. Frech, R. A. Wheeler, *J. Phys. Chem.* **1994**, *98*, 100–110.
- [16] S. Schantz, J. Sandahl, L. Börjesson, L. M. Torell, J. R. Stevens, *Solid State Ionics* **1988**, *28–30 Part 2*, 1047–1053.
- [17] a) C. L. Bender, P. Hartmann, M. Vračar, P. Adelhelm, J. Janek, *Adv. Energy Mater.* **2014**, *4*, 1031863; b) C. L. Bender, W. Bartuli, M. G. Schwab, P. Adelhelm, J. Janek, *Energy Technol.* **2015**, *3*, 242–248.
- [18] H. H. Eysel, S. Thym, *Z. Anorg. Allg. Chem.* **1975**, *411*, 97–102.
- [19] a) J. M. Alía, H. G. M. Edwards, *Vib. Spectrosc.* **2000**, *24*, 185–200; b) A. Brodin, B. Mattsson, K. Nilsson, L. M. Torell, J. Hamara, *Solid State Ionics* **1996**, *85*, 111–120; c) D. W. James, R. E. Mayes, *J. Phys. Chem.* **1984**, *88*, 637–642; d) S. F. Johnston, I. M. Ward, J. Cruickshank, G. R. Davies, *Solid State Ionics* **1996**, *90*, 39–48; e) G. Petersen, P. Jacobsson, L. M. Torell, *Electrochim. Acta* **1992**, *37*, 1495–1497; f) S. Schantz, *J. Chem. Phys.* **1991**, *94*, 6296–6306; g) S. Schantz, L. M. Torell, J. R. Stevens, *J. Chem. Phys.* **1991**, *94*, 6862–6867.

Received: February 15, 2016

Revised: April 23, 2016

Published online: May 30, 2016